

BEAM LOADING COMPENSATION

T. Berenc, B. Chase, J. Dey, K.Koba, I. Kourbanis, K.Meisner, R. Pasquinelli, J. Reid, C. Rivetta, J. Steimel, D. Wildman,

May 5, 2003

Introduction

The issue of beam loading during slip stacking had been described in detail in the Run IIb Plans documents. In this write-up we describe the recent slip stacking simulations using the current rf parameters, the modeling of the MI 53 MHz rf system and recent beam loading measurements.

Simulations

The whole slip-stacking process was simulated with ESME. The 53 MHz cavities were modeled as RLC resonators with an $R_s = 25 \text{ Kohms}$ and $Q = 2500$. The beam loading voltage was calculated in the time domain by using the Green's function for a resonator.

To simulate beam loading compensation using a direct rf feed-back the R_s and Q of each cavity was reduced by the open loop feed-back gain leaving R_s/Q the same. In this case no delay was considered. The feed-forward compensation was simply simulated by reducing the cavity impedance by the amount of the feed-forward compensation gain.

The results of the simulations are summarized below:

- a) No beam loading compensation. The results are shown in Fig.1
- b) Feed-forward only.
In this case we need to reduce the 53 MHz cavity impedance by a factor of 20 (26 db) or more (Fig.2).
- c) Fundamental rf feed-back only.
In this case only fundamental rf feed-back with various gains was considered. A gain of at least 100 (40 db) is required. (Fig. 3)
- d) Feed-back and feed-forward compensation. Using fundamental feed-back with a gain of 5 (14 db) reduces the feed-forward requirements to a gain of 10 (20 db).(Fig. 4).

Based on the simulations results so far we require feed-forward compensation with a gain of 10 (20 db) along with a fundamental feed-back compensation with a gain of 5 (14 db).

In the near future we plan to have a more realistic simulation of the different beam loading compensation schemes by using as an input in ESME the cavity response to a unit current triangular pulse generated by a cavity model that includes all the control loops plus a more realistic description of the the rf feed-back (including cable delays) and feed-forward compensation.

Mean Radius	528.3 m
Synchronous Energy	8938.28 MeV
Transition gamma	21.6
RF peak voltage,each cavity	62 KV
Recapture RF Voltage	1.1 MV
RF harmonic	588
Shunt resistance of 18 cavities	4.5 Mohm
Roaded Q of cavities	2500
Synchrotron frequency (63 KV)	217 Hz
Bucket height	8.2 (MeV)

Table 1: MI rf and beam parameters used in ESME simulations

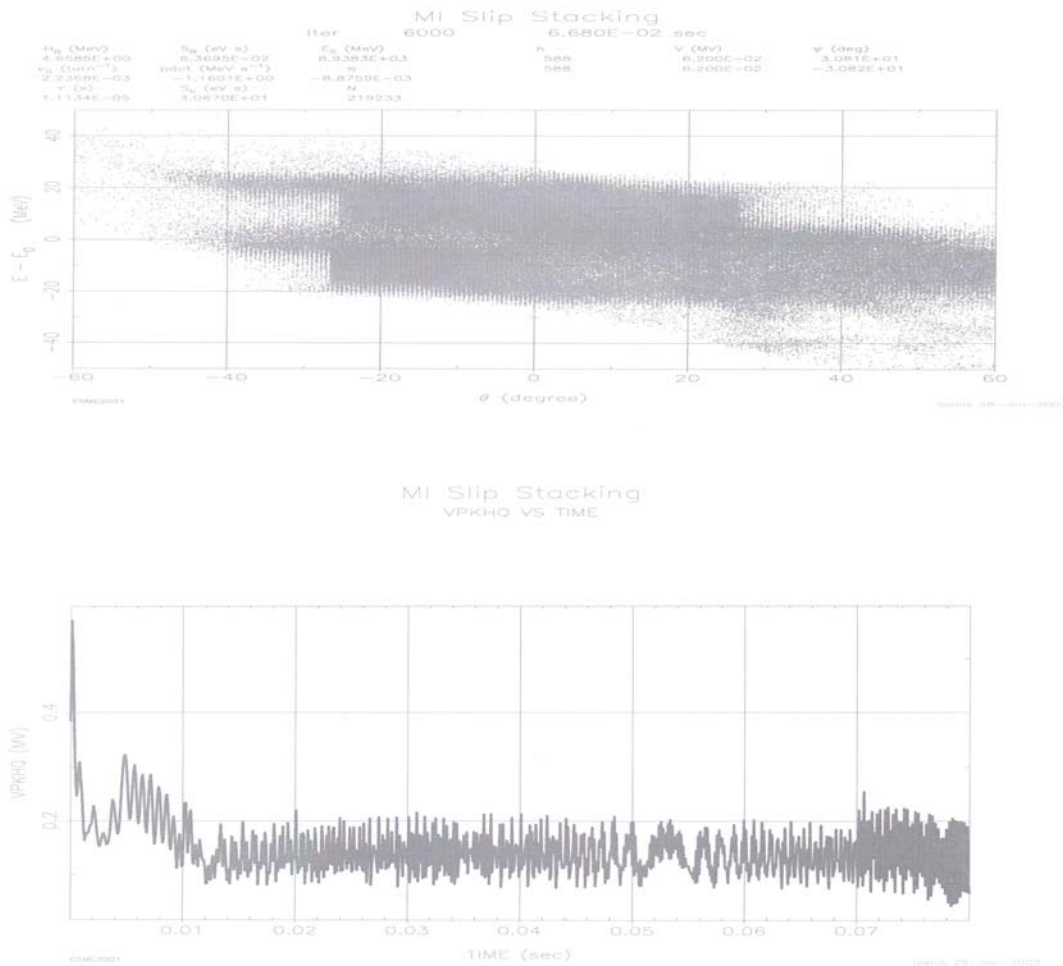


Figure 1: ESME simulation pictures of phase space (top) and beam loading voltage as a function of time(bottom) for 1E13 particles and no beam loading compensation

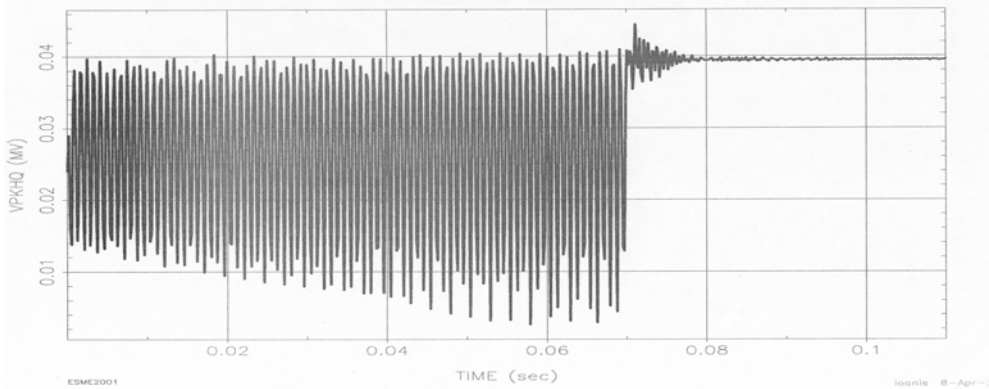
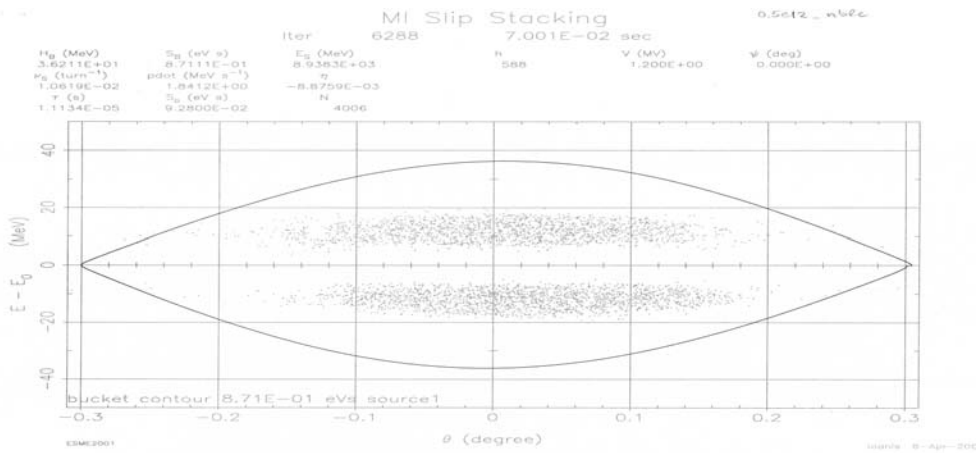
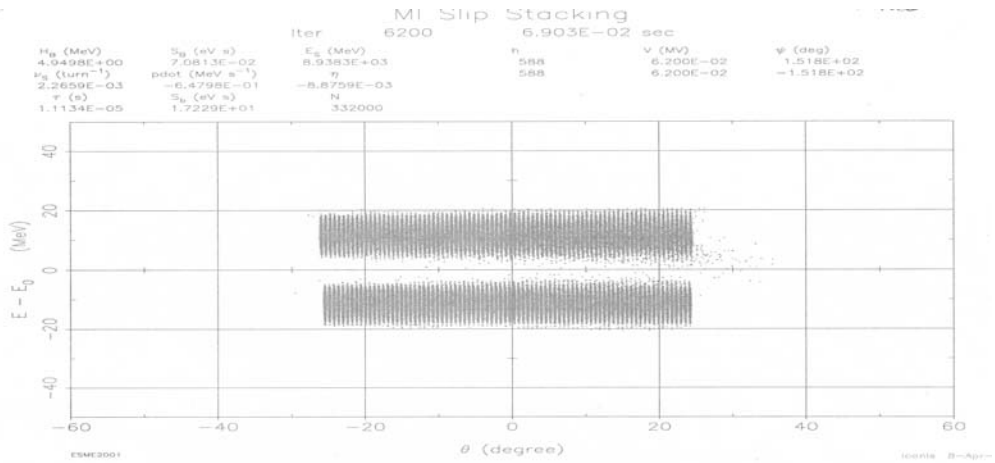


Figure 2: Slip Stacking with $1E13$ particles and 26 db feed-forward compensation. The top picture shows the two batches at the end of slipping while the bottom picture shows the beam induced voltage as a function of time.

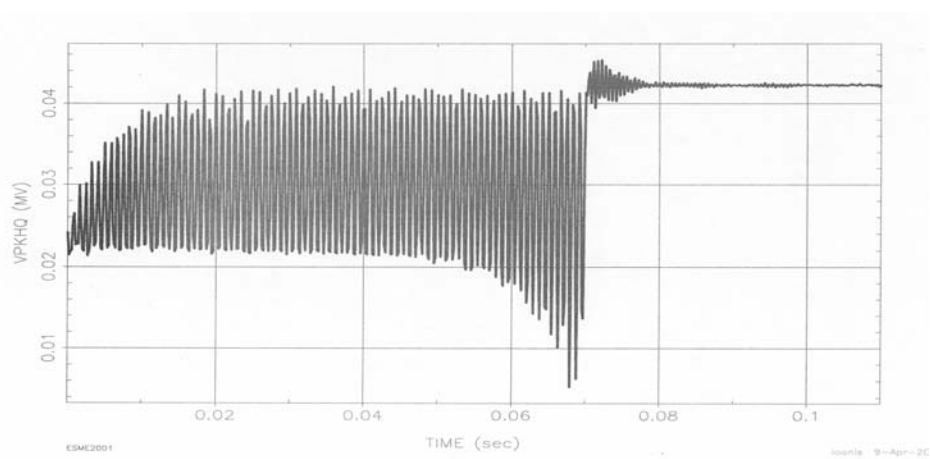
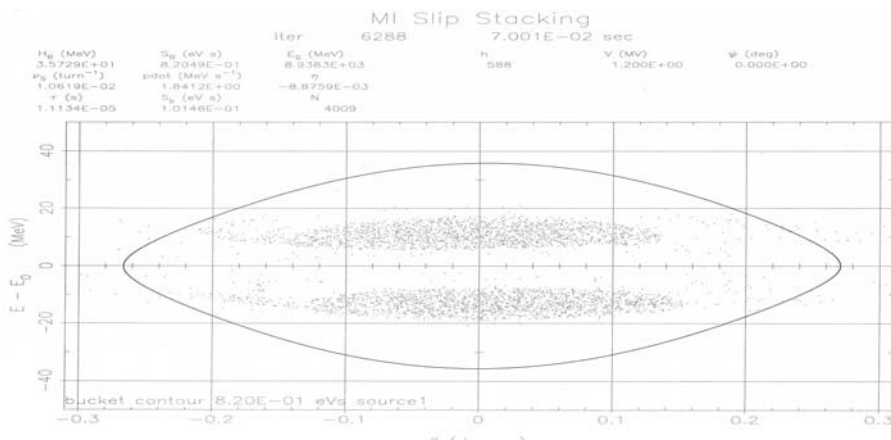
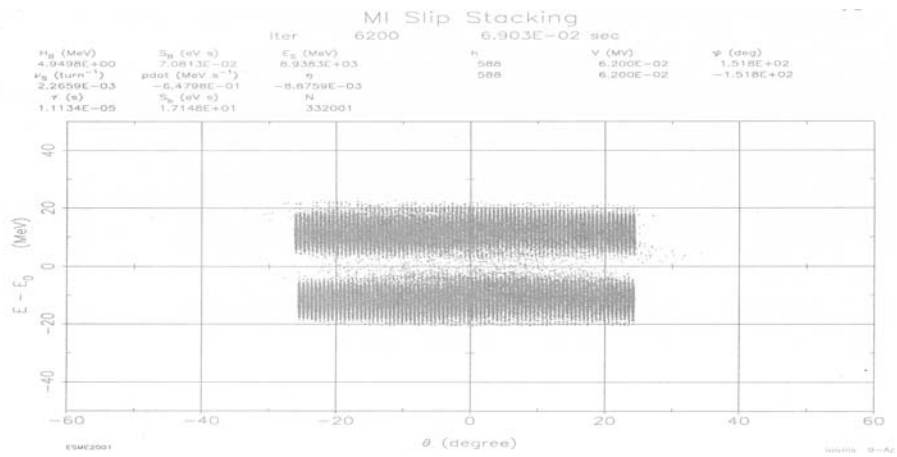


Figure 3: Slip Stacking with 1E13 particles and 40 db of fundamental rf feed-back.

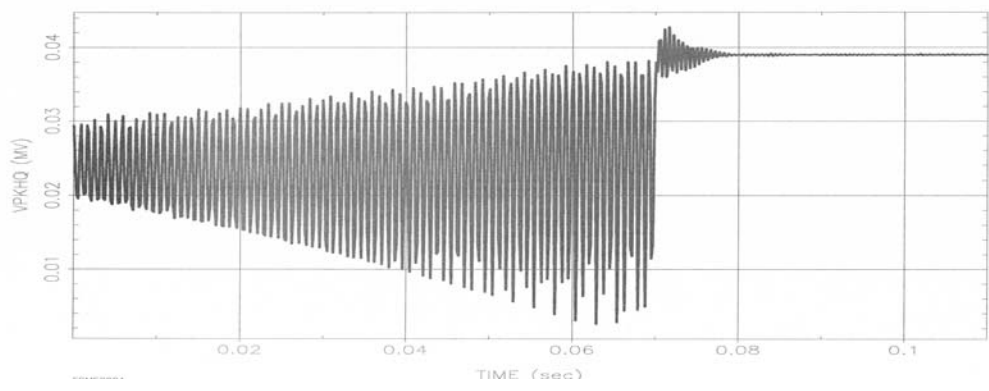
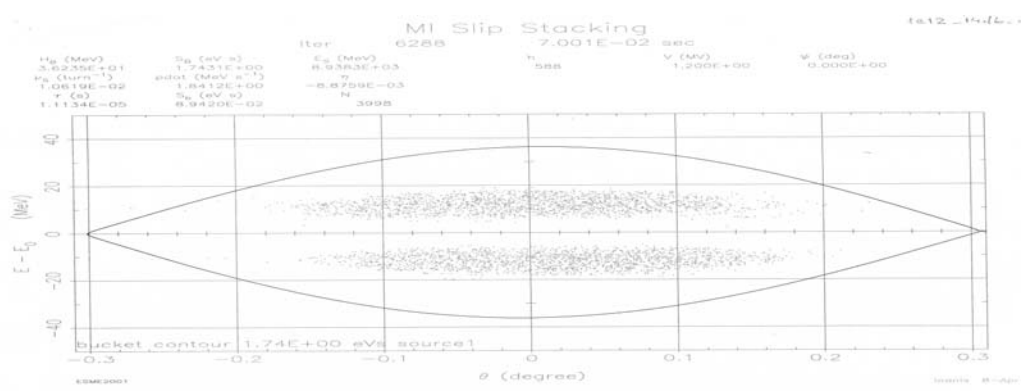
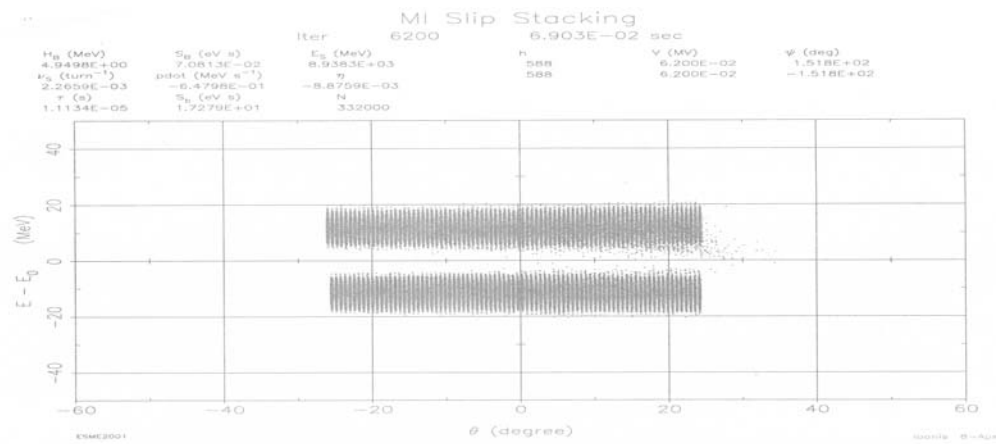


Figure 4: Slip Stacking with 1E13 particles, 14 db of fundamental feed-back and 20 db of feed-forward compensation.

RF System Modeling

In conjunction with performing experimental measurements to determine the RF system's behavior during slip-stacking, a mathematical model of the RF system is being developed. This model is intended to help predict system performance and to aid the design of overall system architecture and subsystem components. It provides a means to understand the deterministic factors and the limitations of the system. Furthermore, if the model can predict present behavior, it can be used as a guide to determine extrapolated performance and upgrade specifications (i.e. required RF drive power and power supply specifications). It can also help to plan and prepare for RF system studies.

One of the key elements of the high-level RF (HLRF) system is the Eimac¹ Y567 (a modified 4CW100000E) tetrode tube which is used to drive the cavities. A simple tube performance calculator that was initially used for the design of the Booster Station 12 solid-state drive RF system has been updated and utilized for analyzing the performance of these same tubes in the MI RF system. This calculator was written in the Matlab² environment. It interpolates and extrapolates the grounded grid constant current curves from Eimac to determine the instantaneous grid, screen, and anode current during cathode-driven, RF grounded-grid operation for any arbitrary load angle and bias condition. It can be used to determine such parameters as the tube's transconductance at the fundamental RF component, cathode drive power requirements, DC bias supply requirements, and delivered RF power. A sample of some simulated parameters which were post-processed in Mathcad³ are shown in Fig.5 and 6.

¹ Eimac is a division of CPI (Communications and Power Industries)
<http://www.cpii.com/eimac/index.html>

² Matlab is written by The Mathworks, Inc., 3 Apple Hill Drive, Natick, MA 01760-2098,
<http://www.mathworks.com>

³ Mathcad is written by Mathsoft, <http://www.mathsoft.com>

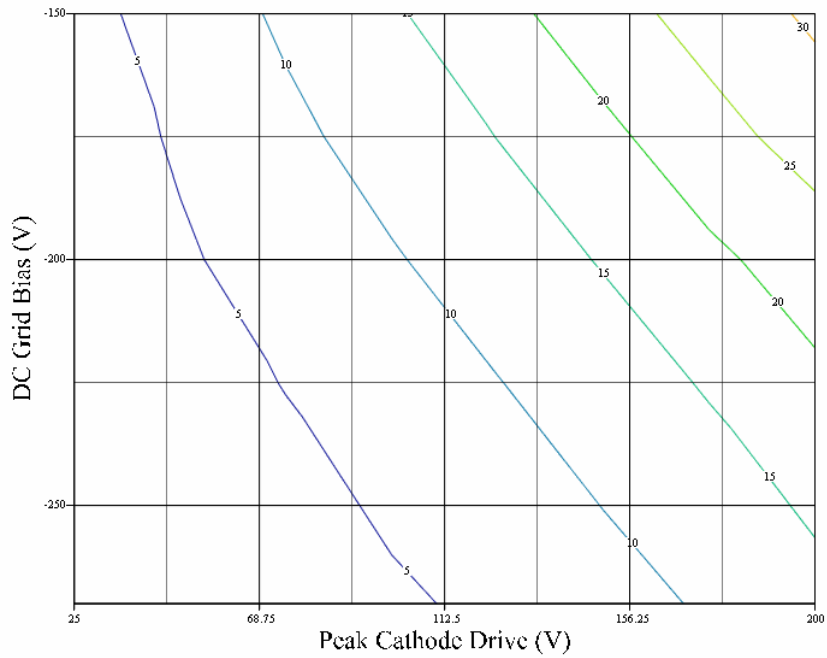


Figure 5: Constant Fundamental RF Anode Current (in Amps) contours as a function of cathode drive and DC grid bias.

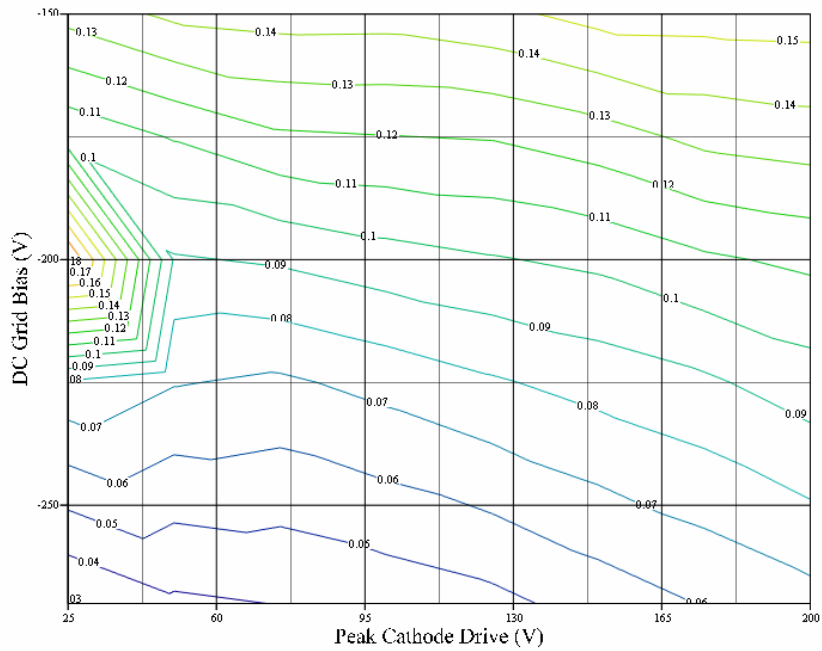


Figure 6: Constant Tube Transconductance contours as a function of cathode drive and DC grid bias. The behavior for low cathode drive near -200V grid bias is due to -200V being the approximate grid bias at which the tube starts to conduct appreciable current.

The common operating conditions used to generate the above graphs were a fixed anode bias of 5 KV, a screen bias of 1.05 KV, and an RF anode voltage swing of 0 V to simulate beam loading compensation on the cavities that are desired to be “off” during slip-stacking. To use the above graphs, one could determine a combination of grid bias and cathode drive that would result in a desired fundamental anode current that compensates for a given level of beam loading. Then given this grid bias and cathode drive level condition determined from Fig.4, the transconductance of the tube is read from Fig.5. This transconductance gives the load on the cathode circuit that is driven by the solid-state driver amplifiers. Thus, the required solid-state drive power can be determined. Of course other parameters determined with the tube performance calculator can determine other system requirements such as DC anode power supply current.

The previous example shows only one scenario for which tube parameters can be determined from the tube performance calculator. The calculator also can be used to simulate other scenarios such as beam-loading compensation in the presence of accelerating voltage; during which the tube must simultaneously supply the current which develops the cavity potential and the current which compensates for beam-loading. Thus, the tube calculator is a very useful tool for determining the demands placed upon the tube amplifier during beam-loading compensation.

Another tool that is being developed to analyze the performance of the RF system is a Matlab Simulink⁴ model which models the dynamic behavior of a single MI RF system with its control loops and beam-loading compensation loops. Figure 7 shows the currently developed model.

⁴ Simulink is a block diagram modeling tool for analyzing continuous and discrete time systems. It is integrated with Matlab.

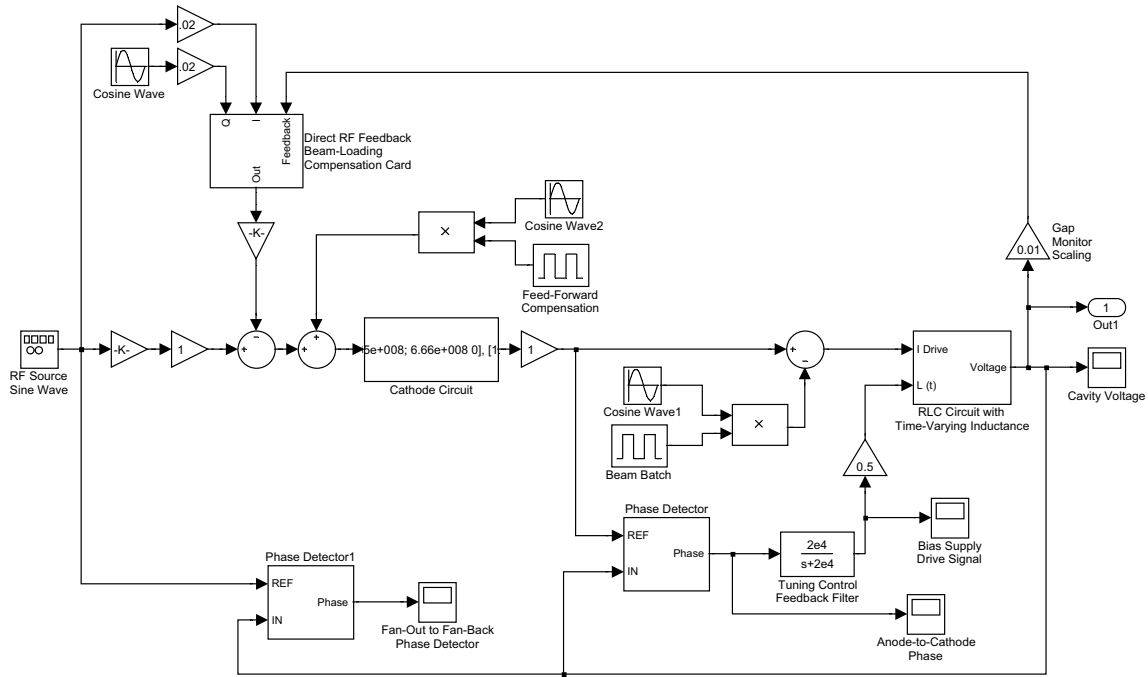


Figure 7: Current Matlab Simulink model of a single MI RF system.

The Simulink model is a composition of various subsystem models. The ferrite tuned MI cavity is modeled as a parallel RLC circuit with a time-varying inductance. The time-varying inductance is used for modeling the dynamic tuning control of the cavity by the ferrite tuners. The feedback tuning controller is currently modeled as a simple lowpass filter (LPF). The cathode resonant circuit of the tetrode tube amplifier is modeled as a bandpass filter (BPF). Both the anode-to-cathode phase-detector sub-block, which is currently used as the cavity tuning monitor, and the fan-out to fan-back phase-detector sub-block consist of a mixer style phase detector with a LPF output. The direct RF beam-loading compensation card sub-block consists of down-converter mixers with LPF's, up-converter mixers, and the actual RF system feedback delay similar to the actual compensation card.

The beam current is shown to enter the system at the cavity. It is modeled as a pulse-wave amplitude-modulated co-sinusoidal signal. This model is justified by the fact that, in essence, the beam batch current in the cavity can be considered to be an impulse train multiplied by a pulse wave. The impulse train consists of impulses separated by the bunch spacing which is equal to an RF period. Thus the impulse is a Fourier series of harmonics of the RF frequency. The pulse-wave has a period of a revolution and a pulse width equal to the batch length. Thus, the pulse wave is a Fourier series of harmonics of the revolution frequency. Assuming that the impedance of the cavity is negligible outside a bandwidth equal to the RF frequency centered at the RF frequency and that the pulse-wave is well represented only by harmonics up to $\frac{1}{2}$ of the RF frequency, then the convolution of the RF harmonics of the impulse train with the fourier representation of the pulse-wave can be neglected. Thus for most practical purposes, the beam batch can be represented as a pulse-wave amplitude-modulated fundamental-RF co-sinusoid whose peak magnitude is twice the DC component of the continuous impulse train.

The feed-forward beam loading compensation is currently modeled identically to the beam signal and enters the system with an opposite sign at the cathode of the tube amplifier. The direct RF feedback signal enters the system at the same place after processing in the compensation card.

An example set of simulation results is shown in Fig. 8. For these results the system model included a direct RF feedback gain of 7 (defined as the open-loop gain around the feedback path), a beam-loading magnitude equivalent to a total of $4E12$ protons distributed evenly into 84

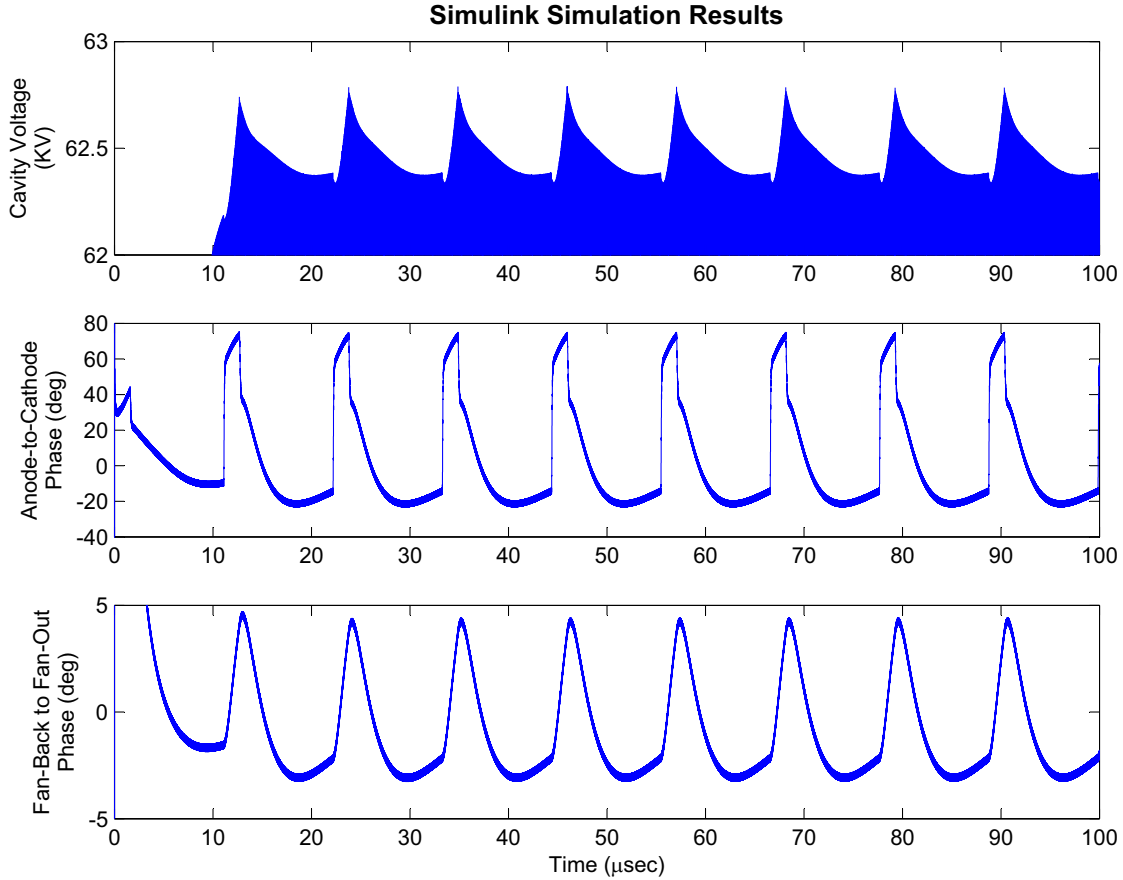


Figure 8: Simulink Simulation Results for conditions of: accelerating voltage of 62.5KV, beam-loading magnitude equivalent to $4E12$ particles in 84 bunches, feed-forward beam-loading compensation of $1/2$ the beam-loading magnitude, direct RF feedback gain=7 (defined as the open-loop gain around the feedback path)

bunches, a feed-forward beam compensation of $1/2$ of the beam-loading magnitude, and a cavity accelerating voltage of 62.5 KV.

There are a few noteworthy observations from the above results for the currently configured RF system. The anode-to-cathode phase detector's average value settles to 0 due to the tuning control loop. This is an average of a complicated signal which consists of sharp fluctuations produced from the feed-forward component being injected into the cathode circuit and other slow time-constant responses of the system. Thus the cavity's average tuning (or de-tuning) is determined by the level of feed-forward compensation. Even if perfect feed-forward compensation was achieved, the anode-to-cathode phase detector would still exhibit such behavior because the anode signal is generated from the sum of all the currents (beam, cavity, and compensation) while the cathode signal is generated from only the cavity and compensation currents. One suggestion for eliminating this complex tuning control behavior is to switch to controlling the cavity tune with the fan-back to fan-out phase detector. This may also help to

control the overall system phase from fan-out to fan-back which is evidently needed from the simulation results shown above.

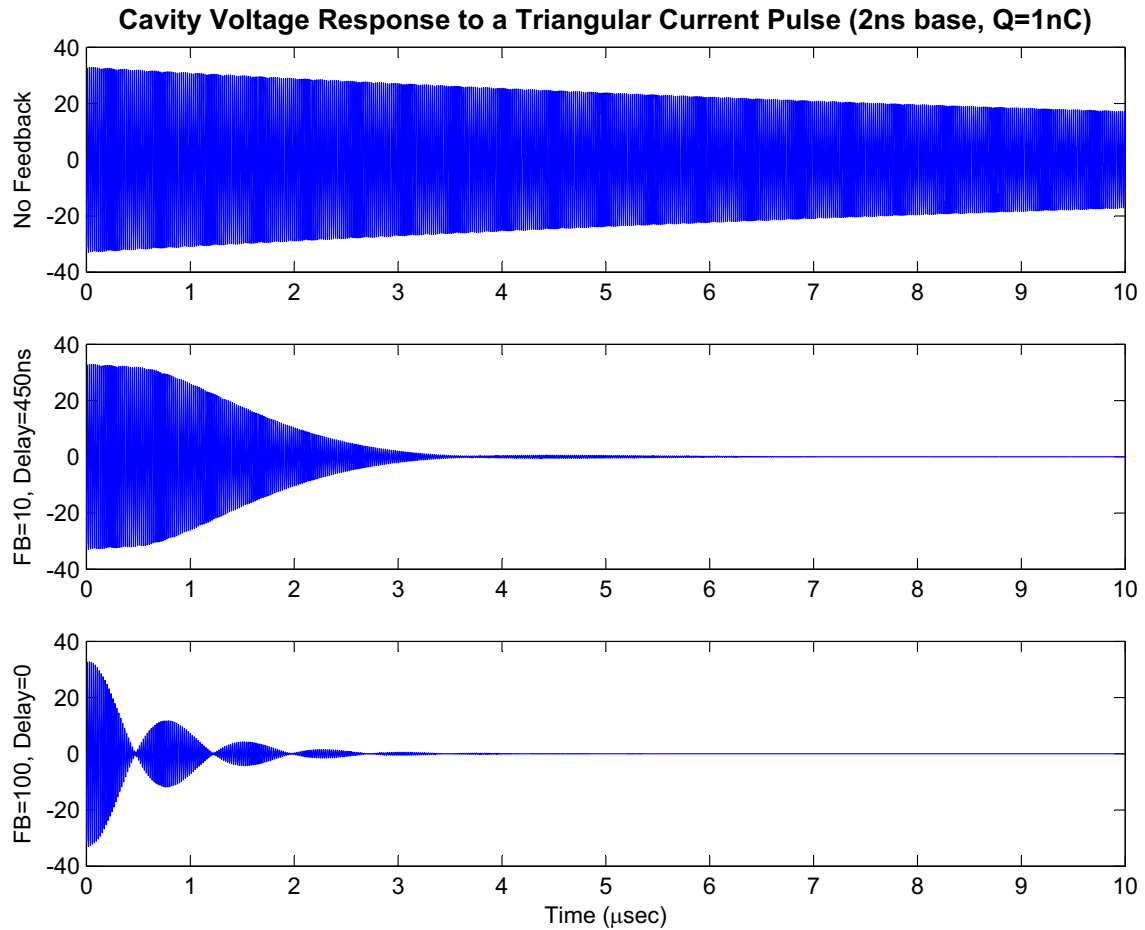


Figure 9: Simulated cavity voltage response to a triangular current pulse with a 2ns base and an integrated charge of 1nC for various system conditions.

Another use for the Simulink model is to provide ESME with the cavity voltage response to a single beam bunch with the various RF system control loops active. This can allow for the inclusion within ESME of a more realistic cavity response. A sample of three different simulated cavity responses to a single bunch are shown in Fig. 9. The bunch current shape was chosen to be a triangular pulse with a 2 ns base width and an integrated charge of 1 nC.

The oscillatory envelope for the last case of no system delay with a feedback of 100 is due to the poles introduced into the system by the LPF's of the direct RF feedback beam-loading compensation card.

Improvements to the RF system Simulink model can include the amplitude regulation loops, a more accurate representation of the actual feed-forward compensation, another beam model to include the second slip-stacking beam batch, and the integration of the tube performance calculator.

Furthermore, in order to simulate over long time scales (i.e. for many batch turns in the machine), envelope equations can be used.

I/Q model of the cavity - Base-band model

The cavity output voltage is a sine-wave signal modulated both in phase and in amplitude. The fundamental frequency is given by the reference frequency of the current driving the cavity. The output voltage can be expressed mathematically as

$$\begin{aligned} v_c(t) &= \text{Re} \left\{ a(t) \cdot e^{i[\omega_d t + \varphi(t)]} \right\} = a(t) \cos \varphi(t) \cos(\omega_d t) - a(t) \sin \varphi(t) \sin(\omega_d t) \\ &= v_{c_i}(t) \cos(\omega_d t) - v_{c_q}(t) \sin(\omega_d t) \end{aligned}$$

where $a(t)$ is the amplitude modulation, $\varphi(t)$ is the phase modulation, and $\omega_d = 2\pi f_d$ is the driving frequency. Due to the high quality factor Q of the resonant cavity, the bandwidth of the modulation signals is much lower than the driving frequency. Stability and performance of the cavity and interactions with the beam are associated with the slow dynamics imposed by the cavity bandwidth on the modulation signals. To design controllers and assess performance and stability of the cavity it is more useful to define a mathematical model that describes the dynamic relation between the input and output modulation signals of the cavity. Assuming the driving current delivered by the radio-frequency tube to the cavity is

$$i_g(t) = i_{g_i}(t) \cos(\omega_d t) - i_{g_q}(t) \sin(\omega_d t)$$

and the beam current component around the driving frequency is

$$i_b(t) = i_{b_i}(t) \cos(\omega_d t) - i_{b_q}(t) \sin(\omega_d t)$$

a model relating the in-phase/quadrature components can be represented as depicted in Fig. 10 .

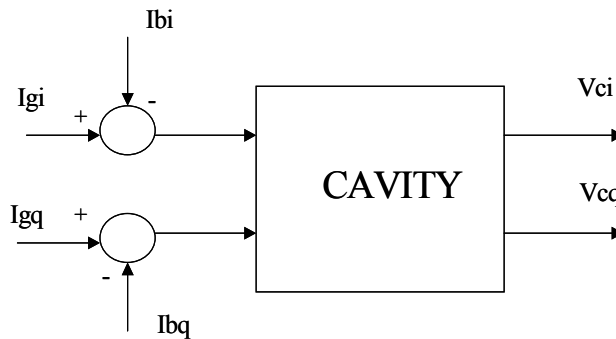


Figure 10: Base band model of the cavity

Some characteristics of this cavity model are:

- a.) The model dynamics depend not only on the cavity parameters but also on the driving frequency f_d .
- b.) When the cavity operates out of resonance, there is cross-coupling between the output - input I/Q components.

To validate the application of this model the responses of the cavity to beam loading and the step response when it operates in closed-loop are shown in Fig.11. In these plots, the response of the base-band model is compared with the response of the cavity in the same conditions but using a model that includes the RF signals.

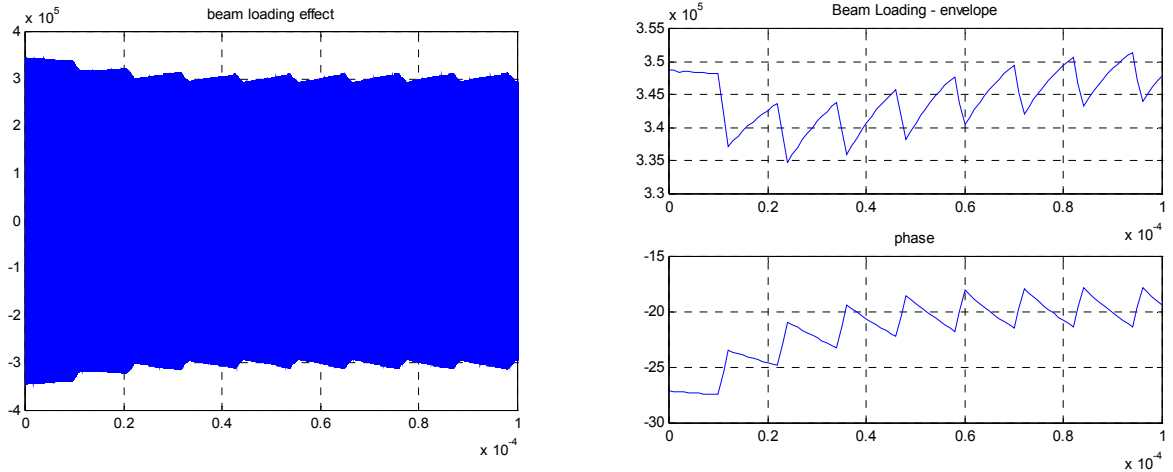


Figure 11a: Beam loading effect on the cavity. Comparison between the response of the cavity using a model that includes the RF frequency and the response using the base-band model .

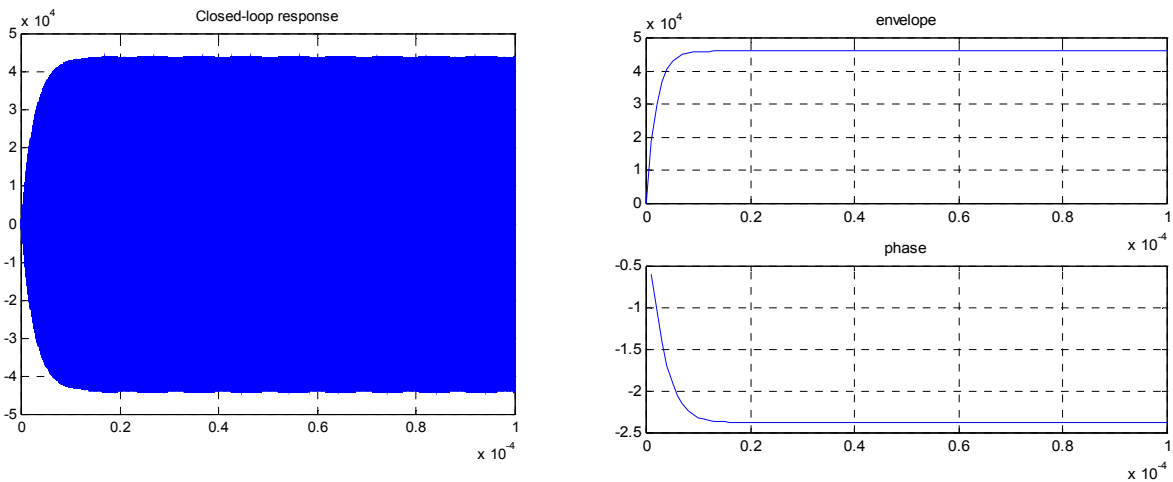


Figure 11b: Closed-loop response of the RF cavity. Comparison between the response of the cavity using a model that includes the RF frequency and the response using the base-band model .

Based on this analysis, the following studies will be conducted in order to assess the performance and stability of the cavity operating under slip stalking:

- a.) Include a variable inductance to address the cavity tuning loop behavior.
- b.) Analyze the perturbing effect of bunched beam currents with frequencies equal and different to the RF frequency.
- c.) Include the beam dynamic into the model
- d.) Design appropriate controllers to reject the beam loading perturbation.

Furthermore, in order to simulate over long time scales (i.e. for many batch turns in the machine), envelope equations can be used.

Current Requirements

The original design specification for the Main Injector was that transient beam loading from 6 E10 protons per bunch will require about 1.25 amps delivered to the cavities, supplied by 15 amps of rf current generated by the power amplifier (12:1 cavity step-up ratio). The MI amplifiers can deliver 200 Kwatts of rf power which at a plate voltage of 20 Kvolts will produce a peak rf current of approximately 21 amps. This is a 40% surplus of current available, which will provide good operating lifetime as the power tube ages. Since the MI started operating, the life of the power tube is approximately 3 years.

The power amplifier is cathode driven (grid grounded for rf purposes) by the solid state driver amplifier so all the rf current must come from the solid state amplifier.

In order to check the solid state driver's available current, a dummy load arrangement was configured as shown in Figure 12.

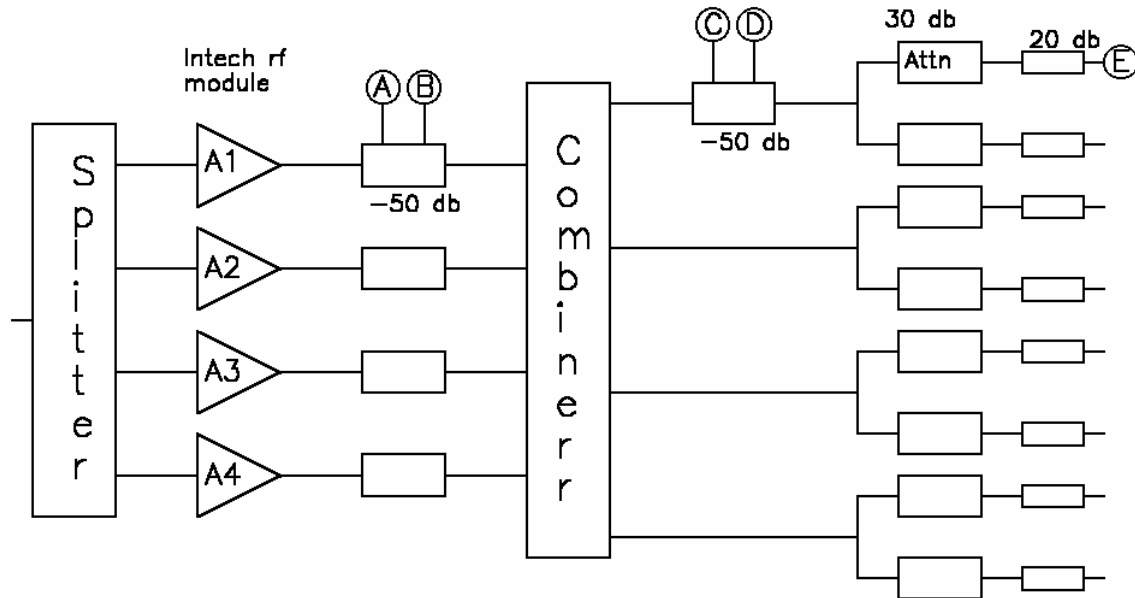


Figure 12: Test set-up for rf current measurements.

Forward Voltage mVpp A	Forward Power Watts A	Reflected Voltage mVpp B	Reflected Power Watts B	VSAR	Forward Voltage mVpp C	Forward Power Watts C	Reflected Voltage mVpp D	Reflected Power Watts D	VSAR	Actual Voltage mVpp E	Actual Voltage Vrms E	Actual Power Watts E	Z Ohms	RF Current Amps rms	DC Current Amps
0.61	93	0.115	3.3		0.65	105	0.18	8		0.46	51.4	53	6.25	8.23	
1.1	302	0.195	9.5		1.14	325	0.325	26.4		0.8	89.4	160	6.25	14.3	
1.7	722	0.307	23.5	1.44:1	1.8	809	0.5	62.5	1.77:1	1.25	140	390	6.28	22.3	144

Table 2. Experimental results

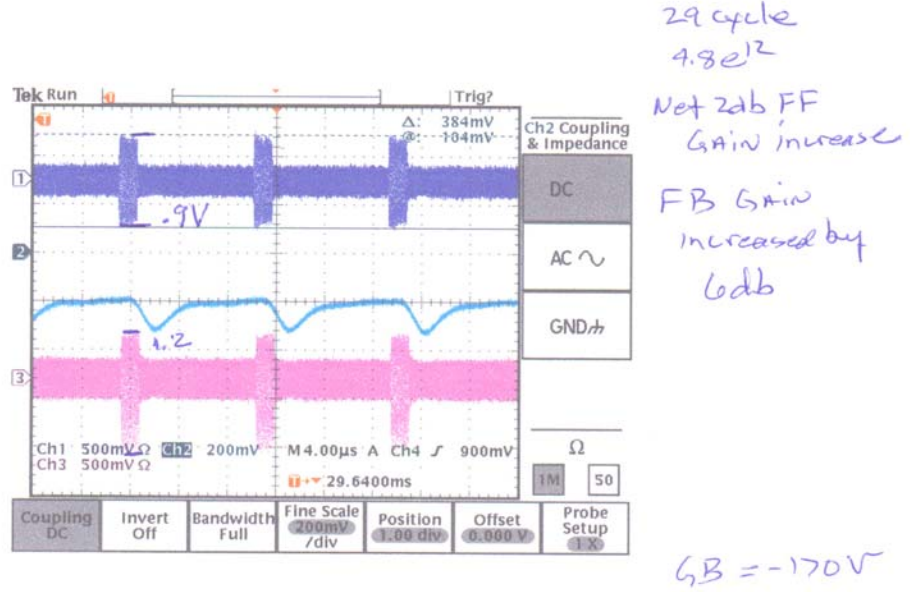
Each load is 50 ohms so with the parallel configuration, the actual load impedance to the combiner is 6.25 ohms. The combiner is matched to 12.5 ohms, the original design specification.

The maximum rf current available as shown from table 2 is 22.3 amps rms. This was achieved with running the solid state amplifiers at 46 V dc and approximately 144 amps dc. The rf amplifiers are rated to run at 48 volts so a bit more current is probably available. We have operated the amplifiers at 46 volts to be conservative and up to this point have not needed to run the amplifiers full out.

It is important to keep in mind that there needs to be at least 40 % headroom to compensate for aging of the power tube.

Since we are going to run the amplifiers in class A for part of the rf cycle, the impedance that the cathode presents to the solid state amplifier is close to 6.25 ohms. If we change the output combiner to match to 6.25 ohms instead of the present 12.5 ohms, a better match is achieved.

The cathode current required to cancel the beam loading voltage on one rf station on a standard MI \$29 stacking cycle with 4.8×10^{12} protons was also measured. The rf station was running in class A operation with feed-forward and rf feed-back compensation active. The cathode current rf current was calculated from the cathode voltage and the forward solid state amplifier power while the amount of the beam loading compensation achieved was estimated from the local station phase detector (fanout to fanback phase).



Cathode rf = $1.2 \times 191 = 229.2V_{pp} = 81V_{rms}$
 Power Forward = $.9 \times 316 = 809watts$
 Cathode Z = $\frac{V^2}{P} = 3.1 \Omega$
 Cathode I = $\frac{V}{Z} = \frac{81}{3.1} = 10Amps$

Figure 13: Cathode rf, forward power and local phase detector for station 1 with 4.8×10^{12} particles and beam loading compensation on.

From the measurements the cathode rf current required to cancel the beam loading on station 1 with $4.8 \text{ E}12$ never exceeded 13 amps. Scaling this to the slip stacking that requires slipping of two batches of $5.0 \text{ E}12$ protons we can assume that we will need at most 27 amps of rf current. Adding a safety factor of 40% to allow for power amplifier aging, the total estimated current need out of the solid state driver is 37.8 amps.

Future Work

Since we have determined the amount of compensation required and the availability of rf current to compensate beam currents up to $8 \text{ E}13$, we plan to concentrate in applying the feed-forward beam loading compensation during the slip stacking. The challenge we are facing is that during slip stacking the rf stations we need to compensate have no rf drive so the application of the beam loading compensation signals must be virtually free of rf leakage. Efforts are in progress to understand and reduce any leakage during the application of the beam loading compensation. In case we are not successful, the other approach is to apply rf drive to all stations but cancel the net amplitude of all stations but the two used for the slip stacking.